Lab on a Chip

Dynamic Article Links

Cite this: *Lab Chip*, 2012, **12**, 1296

www.rsc.org/loc

PAPER

Inertial lift enhanced phase partitioning for continuous microfluidic surface energy based sorting of particles

Vahidreza Parichehreh[a] and Palaniappan Sethu*[b]

Received 25th October 2011, Accepted 9th January 2012
DOI: 10.1039/c2lc21034g

A new microfluidics technique that exploits the selectivity of phase partitioning and high-speed focusing capabilities of the inertial effects in flow was developed for continuous label-free sorting of particles and cells. Separations were accomplished by introducing particles at the interface of polyethylene glycol (PEG) and dextran (DEX) phases in rectangular high aspect-ratio microfluidic channels and allowing them to partition to energetically favorable locations within the PEG phase, DEX phase or interface at the center of the microchannel. Separation of partitioned particles was further enhanced *via* inertial lift forces that develop in high aspect-ratio microchannels that move particles to equilibrium positions close to the outer wall. Combining phase partitioning with inertial focusing ensures selectivity is possible using phase partitioning with sufficient throughput (at least an order of magnitude greater than phase partitioning alone) for application in the clinical and research setting. Using this system we accomplished separation of 15 μm polystyrene (PS) particles from 1–20 μm polymethylmethacrylate (PMMA) particles. Results confirm the feasibility of separation based on phase partitioning and enhancement of separation *via* inertial focusing. Approximately 86% of PS particles were isolated within the PEG phase whereas 78% of PMMA particles were isolated within the DEX phase. When a binary mixture of PS and PMMA was introduced within the device, ~83% of PS particles were isolated in the PEG phase and ~74% of PMMA particles were isolated in the DEX phase. These results confirm the feasibility of this technique for rapid and reliable separation of particles and potentially cells.

Introduction

Cells are usually found as heterogeneous populations in tissues and other physiological samples. Isolation and sorting into sub-populations typically requires an enrichment or separation step. Isolation and analysis of cells and cellular sub-populations from tissue samples like blood has a wide range of applications including in clinical diagnostics, patient monitoring and rare/stem cell isolation.[1–5] In the past few years there has been a significant increase in the demonstration of new microfluidics based technologies for high throughput, high efficiency sorting and separation of cells and microparticles.[6–8] Microfluidics based approaches have been particularly successful in cell sorting as they offer the ability to develop tools comparable to the size of a single cell to exploit physical, chemical and biological differences between different cell types often not possible using conventional systems due to scaling effects. Several microfluidics based approaches have been developed to accomplish separation of cells based upon physicochemical, immunological, and functional properties like magnetic-activated cell sorting[9,10] (MACS), fluorescence-activated cell sorting[11] (FACS), field-flow fractionation[12–14] (FFF), microfluidic aqueous two-phase system[15–17] (μATPS) and inertial focusing.[18–21] MACS and FACS techniques employ conjugated (*e.g.* magnetic beads and fluorescent) antibodies to label cells of interest. The major issue with the use of antibodies is the fact that they initiate unnecessary activation of cells due to the antibody binding event.[22] Moreover, complexities and high cost of these systems prevent a widespread adoption in the research and clinical setting. In the FFF technique, cells with different physical and electrical properties are subject to external forces of different amplitudes inside a microfluidic system. Commonly used external forces for actuation and sorting include optical,[23] magnetic,[10] acoustic,[24] thermal[25] and centrifugal[26] forces. These techniques are also limited due to complexities with integration of external force fields and low throughput.[27]

Two techniques that have shown great promise for passive label-free cell sorting are aqueous two phase separation (ATPS) and inertial focusing. ATPS is a versatile and sensitive method that has been established since the 60s and 70s.[28,29] Normally in the macroscale, ATPS is accomplished using two immiscible polymers like polyethylene glycol (PEG) and dextran (DEX)

[a]*Department of Mechanical Engineering, University of Louisville, Louisville, KY, USA*
[b]*Department of Bioengineering, University of Louisville, 2210 S. Brook Street, 357 SRB, Louisville, KY, 40208, USA. E-mail: p.sethu@louisville.edu; Tel: +1 502 852 0351*

above certain critical concentrations. Separation with ATPS is based on affinity between the cell/particle and the different phases. Cells/particles migration is dictated by the partition coefficient (ΔK) which is a function of various factors including cell/particle size, shape, charge, receptor density, *etc.* ATPS in macroscale is time consuming and is affected by gravitational forces which in turn affect the yield and quality of the separation. In microfluidic ATPS (μATPS), low Reynolds numbers ensure stable laminar flow and lateral migration can be achieved to avoid gravitational effects. Further, the high surface area to volume ratio allows for a larger interface between the two phases for faster continuous flow phase partitioning. A few investigators have demonstrated the use of μATPS for protein purification,[30] blood cell sorting[15,16] and isolation of large plant cell aggregates.[17] However the low flow rate[15,16] (1–10 μL min^{-1}) of sample at the entrance is the major disadvantage of this technique.

Microfluidic devices that exploit inertial forces that develop in circular and rectangular cross-section microfluidic channels in straight or curvilinear arrangements have been developed to accomplish size based cell sorting.[20,21,31,32] Neutrally buoyant rigid microparticles flowing through straight rectangular cross-section channels experience inertial lift force that causes migration to distinct lateral equilibrium positions corresponding with channel geometry. Arrangement in a curvilinear fashion results in generation of secondary Dean's forces which further reduce the number of equilibrium positions.[20] Several studies in circular and rectangular channels have shown that migration of particles to equilibrium positions is purely a function of size.[18–20] Therefore this technique has been successfully used to accomplish size-based separation of particles and biological samples with significant size differences.[21] This technique by itself is limited in terms of cell sorting as there is a significant size overlap between different cell types.

In this study, we demonstrate a new microfluidics based technique that exploits the selectivity of μATPS to accomplish initial separation and focusing capabilities of inertial forces to accomplish high efficiency, high throughput sorting. This technique offers the ability to enable phase partitioning while maintaining high flow rates that ensure sufficient throughput to allow processing of sufficient sample volumes for research and clinical applications. The technique can be applied to sort cells and particles based on differences in surface energy.

Theory

Inertial focusing in microfluidic channels

In 1961, Serge and Silberberg[33,34] demonstrated particle focusing in small channels when they showed that uniformly distributed suspension of neutrally buoyant particles forms a narrow band at $\sim 0.2D$ from the channel walls in a circular channel of diameter D. This effect was replicated in rectangular cross-section microfluidic channels and the forces contributing to particle focusing were explained.[35] Briefly, particles flowing in a microfluidic channel within a rectangular cross-section are constrained along their streamlines due to viscous effects. However, if the particles are comparable in size to the channel cross-section, the parabolic flow profile due to Poiseuille flow results in non-uniform velocities at different locations within the channel causing a shear gradient and inertial lift forces that vary in magnitude and decay towards the channel walls. These lift forces (F_{SL}) direct particles away from the center of the channels towards the channel walls. As particles migrate closer to the walls, the asymmetric wake around migrating particles is disturbed and results in wall induced lift forces (F_{WL}) that push particles away from the wall. Action of oppositely directed lift forces equilibrates particles in four equilibrium positions in low-aspect ratio channels (h:w < 1) and two equilibrium positions in high-aspect ratio channels (h:w > 2)[20,35,36] (Fig. 1). Focusing of particles occurs when the ratio of the particle diameter (a_p) to the characteristic length (L_C), a_p/L_C, is >0.07 as evaluated by Ookawara *et al.*[37] and experimentally validated by Bhagat *et al.*[20] The characteristic length of a system (L_C) can be approximated to the smallest channel dimension. In rectangular cross-section channels, the complexity of forces generated within can be simplified using several assumptions and the net lift force acting on a particle due to the shear gradient can be estimated as a function of particle diameter (a_p), characteristic length (L_C), density of the fluid (ρ) and average flow velocity (U_f) as:

$$F_L = \frac{2\rho U_f^2 a_p^4}{L_C^2}.$$

Bhagat *et al.*[38] also show using the Stokes law, if μ is the dynamic viscosity of the fluid; the channel length required for particle equilibration (focusing) L_I can be determined from the following equation:

$$L_I = \frac{3\pi\mu}{2\rho U_f}\left(\frac{L_C}{a_p}\right)^3$$

Finally, the Reynolds number (Re) determines the smallest size of particles that can be focused within a microfluidic channel of given dimensions. In general the smaller the particle size, the larger the Re to attain focusing.

Phase partitioning

The theory behind phase partitioning has been established since the 60s and 70s and published by Albertson and Baird[28] and

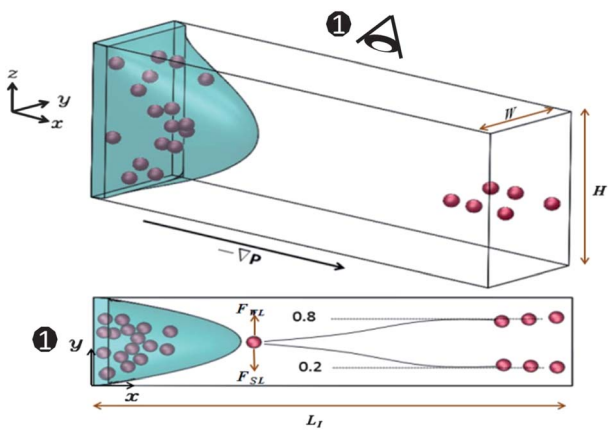

Fig. 1 Schematic of the flow profile and migration of particles to lateral equilibrium position as a consequence of inertial lift forces (F_{SL} and F_{WL}) in straight microfluidic channels with high aspect ratio. AR (h:w > 2 : 1).

Walter *et al.*[29] A mixture of aqueous solution of water soluble polymers like PEG and DEX above critical concentrations forms immiscible liquid two phase systems with a PEG rich layer and a DEX rich layer. DEX and PEG are non-ionic polymers that can be buffered using salts and made isotonic to provide a mild environment for separation of particles while at the same time establishing a potential difference between the two phases. Certain salts like sodium and chloride partition equally whereas other salts like phosphates and sulfates partition unequally resulting in an electrostatic potential difference between the two phases with the PEG phase acquiring a net positive charge and the DEX phase acquiring a net negative charge. The amount of phosphate or sulfate added to the system determines the degree of polarization between the two phases and the resulting electrostatic potential. When particles of a particular surface energy and charge are placed in a two phase system containing PEG and DEX, they interact with the two phases and position themselves in the most energetically favorable location. When particles are placed within such systems they can partition to the PEG phase, the DEX phase or remain at the interface of PEG–DEX (Fig. 2). Movement of particles to any of these locations is a net result of the two forces that act within the system. The first force is the electrostatic force which results from the positively charged PEG and the negatively charged DEX. However, within such systems this force is relatively weak as the electrostatic potentials range in the order of μV and does not significantly influence separation. The dominant force in most phase partitioning studies is the surface energy which is strong enough to move particles/cells to either phase or position them at the interface between the two phases. Each particle/cell type is therefore associated with a partition coefficient which can be defined as:

$$K = \exp\left[\frac{-\Delta E}{kT}\right]$$

where ΔE is the energy necessary for the particle/cell to transfer from one phase compartment to the other (difference in surface energy), k is the Boltzmann constant and T is the absolute temperature. The energy 'ΔE' depends on various factors including particle/cell surface area, surface properties including charge (function of particle/cell surface receptor expression and is usually higher on activated cells) and the concentration of PEG and DEX. Phase partitioning can be enhanced using microfluidics since separations can be accomplished laterally as opposed to vertically thereby eliminating gravitational effects and by exploiting laminar flow to continuously flow the two phases side by side for continuous sorting. The major drawback of microfluidic phase partitioning is the throughput which is not sufficient for processing clinically relevant sample volumes.

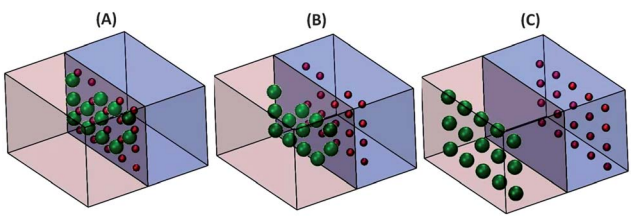

Fig. 2 Illustration of inertia enhanced microfluidic phase partitioning where separation of initially partitioned particles is enhanced by inertial forces that move partitioned particles to equilibrium positions close to the walls. (A) Inlet of the channel, (B) middle of the channel and (C) outlet of the channel.

Materials and methods

Particle suspensions

Sieve-fractionated polymethylmethacrylate (PMMA) particles, labeled with rhodamine, within a size range of 1–20 μm in diameter (less hydrophobic anionic surface) (Microparticles GmbH, Germany) and green fluorescent polystyrene (PS) particles with a diameter of 15 μm (Duke Scientific Corp., Palo Alto, CA, USA) were used for all experiments. Both particles were suspended in deionized water (DI) with 0.5% (w/v) Tween 20 (Fisher Scientific, Florence, KY) and diluted to final concentrations of 3×10^5 and 2.5×10^5 particles mL^{-1} respectively.

Phase partitioning phase

The two-phase polymer system was prepared using PEG (8000, Fisher Scientific, Florence, KY) and DEX (BP1580-100, Fisher Scientific, USA) as described earlier.[15] PEG and DEX were mixed with 1× phosphate buffered saline (PBS) (Fisher Scientific, Florence, KY) at ratios of 4% (w/w) and 5% (w/w) respectively in a 50 mL conical tube and allowed to settle overnight at 25 °C. Following separation of the two phases, PEX and DEX phases were carefully extracted from the top and bottom of the tube respectively using a separate 10 mL pipette as previously described by Soohoo and Walker.[15]

Microfluidic device design and fabrication

The microfluidic device was fabricated using standard soft-lithography procedures and (poly)dimethyl siloxane (PDMS) replica molding *via* modification of a prior design by Hur *et al.*[32] First, a layout of a straight high aspect ratio channel consisting of three inlets, straight channel, expanding region and five outlets was created using L-Edit layout software (Tanner EDA Software, CA, USA). All three inlets had a width of 40 μm and an angle of 35° to produce the optimum laminar flow and prevent mixing at the PEG–DEX interface formation. The width, height and length of the channel were designed to be 40 μm, 95 μm and 5 cm respectively to ensure maximum particle sorting. The length of the expanding region was 2100 μm from the end of the straight segment that gradually increased 3° per 150 μm. Each outlet channel was designed as a 50 μm wide, 2 cm long serpentine fluidic resistor to provide high fluidic resistance and minimize flow distortion due to the irregularities of the syringe pump and particle transport through the outlets. The layout was printed as a dark-field mask (Fineline Imaging, Colorado Springs, CO, USA) and used to define features on 4″ silicon wafers coated with SU-8 100 (Microchem, Newton, MA, USA) using ultraviolet (UV) light exposure. Finally, the features on the silicon wafers were developed and used as negative replica molds for fabrication of the channel structures. The structures were molded using PDMS (Dow Corning, Midland, MI, USA) by mixing the pre-polymer with the cross-linking agent in a ratio of 10 : 1 and baking in an 80 °C oven for 3 h. Following molding, the channels were cut out

from the silicon wafer, access holes were punched and irreversibly bonded after treatment with oxygen plasma in a plasma asher (Nordson March Instruments, Amherst, OH, USA). Inlet and outlet tubings were then press fitted prior to use (Fig. 3).

Setup for focusing of particles

Prior to phase partitioning experiments in high aspect ratio microchannels the optimal flow rates for focusing both PS and PMMA microparticles at two lateral equilibrium positions within the channel were determined. This was accomplished by injecting PMMA and PS microparticles in DI water into the main focusing channel. Samples and DI water were loaded into 10 mL glass syringes (Becton–Dickinson). All syringes were connected to Tygon micro bore PVC tubing (Smallparts, USA) 0.01 inner diameter and 0.03 outer diameter using a 1/2″ luer needle (Smallparts, USA). Syringes containing each sample and DI water were interfaced with the microfluidic device *via* the inlets and were assembled onto separate syringe pumps (Harvard Apparatus, PHD 2000 or Harvard Apparatus, 11 plus). To avoid particle sedimentation, the pump containing the particles was held vertically while DI water pumps were placed horizontally. Sample was injected into the center of the high aspect channel and flanked on both sides by DI water and the movements of particles were monitored in real time using an inverted microscope (ECLIPSE, TE2000-U, Nikon, Tokyo, Japan) equipped with a 12 bit QIMAGING camera (RTIGA-2000R, Canada). High-speed videos and images of particle positioning within the channel were performed at the inlet and outlet and analyzed using Metamorph software (Molecular Devices, Sunnyvale, CA, USA) (Fig. 4). For subsequent phase partitioning experiments the same procedure was followed except that the focusing streams of DI water were replaced by PEG and DEX solutions. Finally the recovered particles were counted *via* the hemocytometry method under the microscope while excitation/emission of PS particles is 468/508 nm (blue/green) and that of PMMA particles is 560/584 nm.

Data collection and reporting

All results for particle counts are expressed as the mean number of particles collected at each outlet as counted using a standard hemocytometer under a fluorescent microscope ± standard error of means (SEM). The results represent a sample size of $n = 3$.

Results

Inertial focusing of particles

To characterize the ability of the fabricated device to accomplish inertial focusing at two equilibrium positions, both PS and

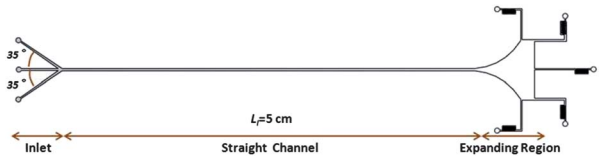

Fig. 3 Layout of the microfluidic device used for all experiments. The device consists of three inlets, straight channel, expanding region and five outlets for particle separation. (Image is not to scale.)

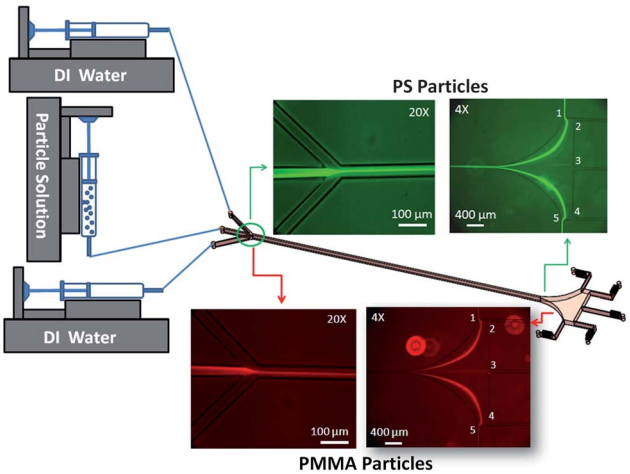

Fig. 4 Microscope images of the inlet and expanding region of the microdevice showing the initial phase partitioning and subsequent inertial focusing of fluorescent polystyrene (PS) and polymethylmethacrylate (PMMA) particles that were introduced at the midpoint of the channel flanked on both sides by DI water to determine the optimum flow rates for focusing. (Solutions and sample at the inlets were introduced at a flow rate of 50 µL min^{-1} resulting in a main channel flow rate of 150 µL min^{-1}.)

PMMA microparticles were separately introduced into the high aspect ratio microchannel at a flow rate (Q) between 30 and 100 µL min^{-1} from the center inlet while DI water was flowed in *via* the two side inlets at a flow rate of 30–100 µL min^{-1} and Re = 22–74 in the straight channel (5 µL min^{-1} increments), such that the particle stream was introduced in the midpoint of the channel flanked on both sides by DI water to determine the optimum flow rates that would allow focusing in the z-direction at lateral equilibrium positions. For particle flow rate between 30 and 100 µL min^{-1} and the same flow rates of DI water, both PMMA and PS particles were separated into two lateral equilibrium positions. However, the maximum yield was derived when the flow rate in all three inlets (sample and 2 DI water inlets) was 50 µL min^{-1} (total flow rate: 150 µL min^{-1}). For PS particles, 98% of particles introduced at the inlets were recovered in outlets 1 and 5 establishing adequate proof that inertial focusing and separation of particles can be accomplished. The remaining 2% of particles collected at the inlet 3 and analyzed *via* microscopy show significant clumping. PMMA particles were isolated at a lower efficiency; ~90% of PMMA particles were recovered at two inlets 1 and 5. All particles collected at the outlets 2, 3 and 4 were the smaller diameter PMMA particles (<5 µm) which require channel redesign to attain focusing (Fig. 4).

Individual particle focusing in two phase flow

To determine if surface energy based interactions dictate the direction of particle migration in two phase systems and to obtain ideal flow conditions for high efficiency focusing of both PS (slightly hydrophobic) and PMMA (slightly hydrophilic), we introduced both types of particles at the center of a two phase flow of PEG and DEX. Since PEG and DEX solutions have different viscosities, the ratio of flow rates necessary to ensure equal distribution within the channel was determined and found

to be ~4.7 : 3. PS particles are hydrophobic and have a greater affinity to the PEG phase whereas the less hydrophobic PMMA particles have a greater affinity to the DEX phase. Once the particles partition to either phase, inertial lift forces within the high-aspect ratio channel enhance the initial separation and move the particles closer to lateral equilibrium positions close to the outer wall. For PS particles, the highest efficiency separation was accomplished when the particle suspension, PEG and DEX flow rates were 85, 65 and 40 μL min^{-1} respectively. Under this condition, ~86% of the PS particles were recovered at inlet 1 (PEG side). For PMMA particles, the highest efficiency separation was accomplished when the inlet flow rates were 80, 60 and 35 μL min^{-1} for sample, PEG and DEX respectively. At these flow rates 78% of PMMA particles were separated at outlet 5 (DEX side) (Fig. 5).

Separation of the binary mixture of PMMA and PS particles

Finally to demonstrate the ability to separate particle mixtures, PS and PMMA particles were mixed at concentrations of 2×10^5 and 1.5×10^5 particles mL^{-1} respectively and introduced into the device at a flow rate of 80 μL min^{-1} while the PEG and DEX flow rates were maintained at 60 and 40 μL min^{-1}. Separation of the PS particles within the PEG phase and PMMA particles within the DEX phase at inlets 1 and 5 respectively was accomplished at an efficiency of 83% for PS particles and 74% for PMMA particles which is consistent with the results obtained using single particle solutions (Fig. 6A and B). To demonstrate that inertial forces significantly enhance initial separation achieved due to phase partitioning we repeated the same experiment at extremely low flow rate (DEX: 1 μL min^{-1}, PEG: 1.5 μL min^{-1} and sample: 5 μL min^{-1}). Since the inertial force (F_L) is proportional to the square of the total flow rate as discussed in the Theory section, the inertial forces acting on the particles are ~600 times smaller than with the inertial focusing enhanced phase partitioning. Results (Fig. 6C) clearly indicate that for the same device at lower flow rates, where inertial forces are insignificant in comparison with the previous experiments, the separation efficiency is significantly reduced. At outlets 1 and 5 ~45 to 50% of PS and PMMA beads were fractionated with ~15% contamination (Fig. 6D). This efficiency can potentially be improved by designing a longer channel for phase partitioning based particle fractionation with extremely small sample inlet stream width (1 particle diameter) and several outlets for fractionation. These modifications will significantly affect sample throughput which is important in real life cell sorting applications in the research and clinical setting.

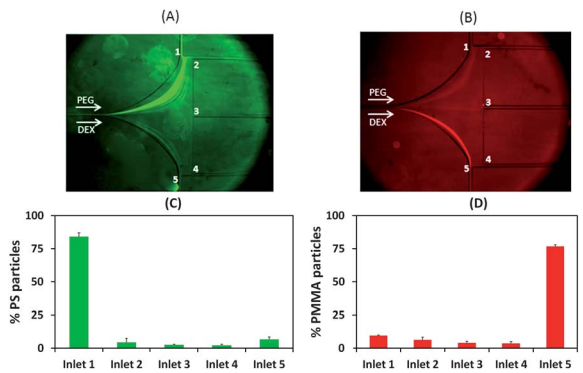

Fig. 5 (A) Separation of PS particles *via* partitioning to the PEG layer. (B) Separation of PMMA particles *via* partitioning to the DEX layer. Particle counts obtained *via* hemocytometry confirming feasibility of separation of (C) PS particles and (D) PMMA particles when introduced at the interface of PEG and DEX solutions.

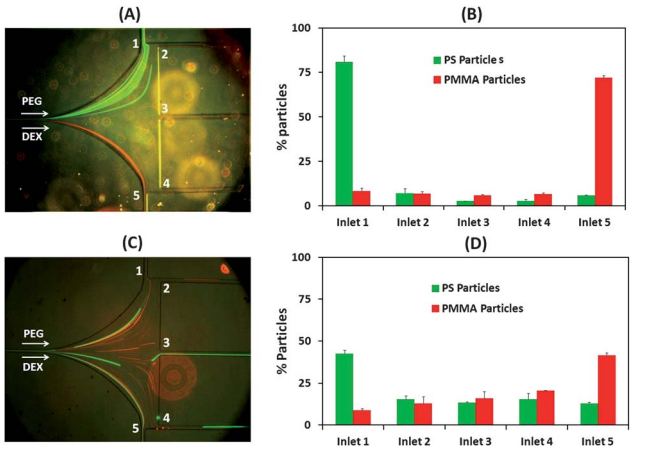

Fig. 6 Inertial force enhanced phase partitioning. (A) Separation of the binary mixture of PS and PMMA particles and (B) particle counts obtained *via* hemocytometry showing separation of PS and PMMA particles which were introduced as a mixture at the inlet at the interface of PEG and DEX streams. (C and D) Control experiments showing separation of the binary mixture of PS and PMMA particles relying on phase partitioning alone in the absence of inertial focusing using the same device.

Discussion

In this study for the first time we demonstrate proof of concept of the ability to cause initial separation using phase partitioning and then enhance the sorting using inertial focusing. Results confirm >1 order of magnitude separation using our technique in comparison to phase partitioning alone. We show separation of particles with different surface energies. This was accomplished with particle concentrations similar to those seen in physiological samples and in high throughput fashion. Using this technique the sample flow rate was ~80 μL min^{-1} which is significantly better than the previously reported sample flow rates of 1 and 10 μL min^{-1} [15,16] without significant need for sample dilution. These results confirm feasibility of this technique as a rapid and reliable separation tool for cell separations for different applications in the research and clinical setting. However, it is important to note that direct translation of these results to cells needs careful consideration of the fact that cells are heterogeneous in nature and properties like surface charge/energy can dynamically vary based on the environment and other factors. Potential clinical and research applications include the sorting of activated leukocytes and circulating tumor cells (CTCs) that have been shown to have differential phase partitioning coefficient from other WBCs and sorting should be feasible using this technique.[39] Sorting of activated leukocytes has several clinical applications particularly in the monitoring of the inflammatory status of individuals with infections and disease whereas the isolation and detection of CTCs has applications in early

detection of cancer and in the monitoring of patients with cancer to develop appropriate treatment strategies.[40–43] Despite unparallel specificity, antibody based approaches can cause activation of cells and initiate unwanted signalling compromising the quality of information that can be attained from cells. Therefore there has been a great emphasis on label-free techniques for cell sorting particularly in cases where monitoring of the immune and inflammatory status of cells is of importance. Phase partitioning of cells and particles in two-phase flows has been applied for cell separations for several years as a label-free alternative to antibody based methods relying on differences in cell surface energy to accomplish separation. Examples of cell populations that can be separated *via* phase partitioning include activated leukocytes and CTCs. However, widespread application has been limited due to the long processing time necessary to attain clear separation and the poor resolution due to gravitational effects. Miniaturization of this process *via* the use of microfluidic channels eliminates the effects of gravity by exploiting laminar flow where the two phases flow side by side; however throughput is extremely low and therefore not suitable for applications in the clinical or research setting. Inertial focusing on the other hand is a high throughput protocol that can accomplish focusing of cells and particles within microfluidic channels with selection being a function of cell/particle size. Inertia enhanced phase partitioning described in this article is one technique that can be used as an alternative to isolate cell populations that differ in surface energy including activated and rare cell populations in a rapid and label-free format. Reliance on cell surface energy eliminates the need for antibody-based labeling and the use of inertial forces to enhance sorting allows sufficient sample processing capabilities to accomplish sorting of clinically relevant samples.

Conclusions

In summary we developed a new microfluidic phase partitioning technique that exploits inertial focusing effects in microfluidic channels to enable high throughput sorting of particles/cells based on differences in surface energy properties. Proof of concept studies demonstrate the ability to sort PS and PMMA particles using a PEG/DEX two phase system.

Acknowledgements

This work was supported in part by the National Science Foundation under Grant no. 0814194 and a Proof-of-concept Research Grant from the Office of Technology Transfer, Vice President of Research, University of Louisville. The authors would also like to thank Dr Rosendo Estrada and Dr Mostafa Shakeri for valuable help and useful discussions.

References

1 A. Manz and H. Becker, *Microsystem Technology in Chemistry and Life Sciences*, Springer, Berlin, New York, 1999.
2 M. Toner and D. Irimia, *Annu. Rev. Biomed. Eng.*, 2005, **7**, 77–103.
3 H. Odegaard, *Water Sci. Technol.*, 1998, **37**, 43–53.
4 G. Blankenstein and U. Darling Larsen, *Biosens. Bioelectron.*, 1998, **13**, 427–438.
5 P. T. Sharpe and K. Shimura, *Methods of Cell Separation*, Kagako Dozin, Tokyo, 1988.
6 H. Tsutsui and C. M. Ho, *Mech. Res. Commun.*, 2009, **36**, 92–103.
7 P. Chen, X. Feng, W. Du and B. F. Liu, *Front. Biosci.*, 2008, **13**, 2464–2483.
8 X. C. Xuan, J. J. Zhu and C. Church, *Microfluid. Nanofluid.*, 2010, **9**, 1–16.
9 M. Berger, J. Castelino, R. Huang, M. Shah and R. H. Austin, *Electrophoresis*, 2001, **22**, 3883–3892.
10 K. H. Han and A. B. Frazier, *Lab Chip*, 2006, **6**, 265–273.
11 P. S. Dittrich and P. Schwille, *Anal. Chem.*, 2003, **75**, 5767–5774.
12 S. K. Williams and D. Lee, *J. Sep. Sci.*, 2006, **29**, 1720–1732.
13 R. D. Sanderson, F. A. Messaud, J. R. Runyon, T. Otte, H. Pasch and S. K. R. Williams, *Prog. Polym. Sci.*, 2009, **34**, 351–368.
14 N. Pamme and A. Manz, *Anal. Chem.*, 2004, **76**, 7250–7256.
15 J. R. Soohoo and G. M. Walker, *Biomed. Microdevices*, 2009, **11**, 323–329.
16 M. Tsukamoto, S. Taira, S. Yamamura, Y. Morita, N. Nagatani, Y. Takamura and E. Tamiya, *Analyst*, 2009, **134**, 1994–1998.
17 M. Yamada, V. Kasim, M. Nakashima, J. Edahiro and M. Seki, *Biotechnol. Bioeng.*, 2004, **88**, 489–494.
18 D. Di Carlo, *Lab Chip*, 2009, **9**, 3038–3046.
19 I. Papautsky, A. A. S. Bhagat and S. S. Kuntaegowdanahalli, *Microfluid. Nanofluid.*, 2009, **7**, 217–226.
20 A. A. Bhagat, S. S. Kuntaegowdanahalli and I. Papautsky, *Lab Chip*, 2008, **8**, 1906–1914.
21 W. C. Lee, A. A. Bhagat, S. Huang, K. J. Van Vliet, J. Han and C. T. Lim, *Lab Chip*, 2011, **11**, 1359–1367.
22 B. Roda, P. Reschiglian, A. Zattoni, F. Alviano, G. Lanzoni, R. Costa, A. Di Carlo, C. Marchionni, M. Franchina, L. Bonsi and G. P. Bagnara, *Cytometry, Part B*, 2009, **76**, 285–290.
23 M. P. MacDonald, G. C. Spalding and K. Dholakia, *Nature*, 2003, **426**, 421–424.
24 A. Nilsson, F. Petersson, H. Jonsson and T. Laurell, *Lab Chip*, 2004, **4**, 131–135.
25 J. Janca, I. A. Ananieva, A. Y. Menshikova and T. G. Evseeva, *J. Chromatogr., B: Anal. Technol. Biomed. Life Sci.*, 2004, **800**, 33–40.
26 J. Kim, S. Hee Jang, G. Jia, J. V. Zoval, N. A. Da Silva and M. J. Madou, *Lab Chip*, 2004, **4**, 516–522.
27 B. Roda, A. Zattoni, P. Reschiglian, M. H. Moon, M. Mirasoli, E. Michelini and A. Roda, *Anal. Chim. Acta*, 2009, **635**, 132–143.
28 P. A. Albertsson and G. D. Baird, *Exp. Cell Res.*, 1962, **28**, 296–322.
29 H. Walter, T. J. Webber, J. P. Michalski, C. C. McCombs, B. J. Moncla, E. J. Krob and L. L. Graham, *J. Immunol.*, 1979, **123**, 1687–1695.
30 R. J. Meagher, Y. K. Light and A. K. Singh, *Lab Chip*, 2008, **8**, 527–532.
31 H. A. Nieuwstadt, R. Seda, D. S. Li, J. B. Fowlkes and J. L. Bull, *Biomed. Microdevices*, 2011, **13**, 97–105.
32 S. C. Hur, N. K. Henderson-MacLennan, E. R. McCabe and D. Di Carlo, *Lab Chip*, 2011, **11**, 912–920.
33 G. Serge and A. Silberberg, *Nature*, 1961, **189**, 209–210.
34 G. Serge and A. Silberberg, *J. Fluid Mech.*, 1962, **14**, 136–157.
35 A. Russom, A. K. Gupta, S. Nagrath, D. Di Carlo, J. F. Edd and M. Toner, *New J. Phys.*, 2009, **11**, 075025, DOI: 10.1088/1367-2630/11/7/075025.
36 D. Di Carlo, D. Irimia, R. G. Tompkins and M. Toner, *Proc. Natl. Acad. Sci. U. S. A.*, 2007, **104**, 18892–18897.
37 S. Ookawara, R. Higashi, D. Street and K. Ogawa, *Chem. Eng. J.*, 2004, **101**, 171–178.
38 A. A. S. Bhagat, S. S. Kuntaegowdanahalli and I. Papautsky, *Microfluid. Nanofluid.*, 2009, **7**, 217–226.
39 H. Walter, L. L. Graham, E. J. Krob and M. Hill, *Biochim. Biophys. Acta*, 1980, **602**, 309–322.
40 S. Suresh, *Acta Biomater.*, 2007, **3**, 413–438.
41 J. Guck, S. Schinkinger, B. Lincoln, F. Wottawah, S. Ebert, M. Romeyke, D. Lenz, H. M. Erickson, R. Ananthakrishnan, D. Mitchell, J. Kas, S. Ulvick and C. Bilby, *Biophys. J.*, 2005, **88**, 3689–3698.
42 S. E. Cross, Y. S. Jin, J. Rao and J. K. Gimzewski, *Nat. Nanotechnol.*, 2007, **2**, 780–783.
43 M. Cristofanilli, G. T. Budd, M. J. Ellis, A. Stopeck, J. Matera, M. C. Miller, J. M. Reuben, G. V. Doyle, W. J. Allard, L. W. Terstappen and D. F. Hayes, *N. Engl. J. Med.*, 2004, **351**, 781–791.